Quantification of Methane-Induced Asphaltene Precipitation in a Multiple Contact Process

He Zhang, Yong Liu, Peihui Han, Shuoshi Wang,* Huarong Yan, Ping Guo,* Jiang Zhang, Zhenqiang Bai, Zhouhua Wang, Haoxiang Hukuang, and Xuyang Li
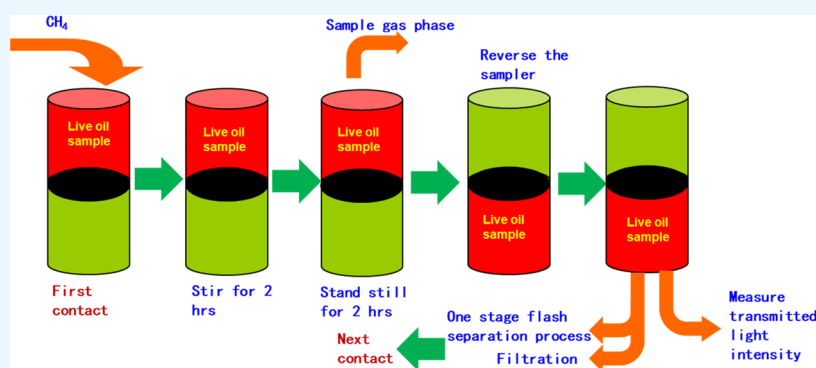
ACCESS | Metrics & More | Article Recommendations

ABSTRACT: A unique experiment design is proposed to study the asphaltene precipitation caused by multiple contact processes during gas injection. The newly proposed experiment quantified the asphaltene precipitation at different methane contact steps. Twenty times methane contacts and corresponding asphaltene precipitation states are measured using a light scattering setup under reservoir condition. The amount of the asphaltene precipitation, the composition changes, and the physical properties changes are measured for the 20 times methane contacts. After verifying the asphaltene precipitation in the static experiments, the formation damage caused by the asphaltene precipitation is studied by core flooding tests for three different permeability cases. We found that the primary asphaltene precipitation mechanism in the multiple contact process during methane injection is not the composition change caused by methane extraction. The methane-induced asphaltene stability loss during the multiple contact process is vital. The size and the structure of asphaltene precipitation particles in the crude oil change with the methane contacts. We found that the mechanism of permeability reduction caused by asphaltene precipitation is different depending on the porous media pore throat size and the asphaltene precipitation particle size. Under our experimental condition, the asphaltene precipitation acts as a conformance control method, leading to well-distance optimization considerations in field applications.

1. INTRODUCTION

Crude oil is mainly composed of various fractions such as saturates, aromatics, resins, and asphaltenes.[1−4] Organic solid deposition in crude oil has always been a severe problem faced by the petroleum industry, and it appears in all aspects of petroleum production and processing. Natural depletion, water injection, and gas injection are all accompanied by asphaltene deposition. Before the interference of the reservoir, asphaltenes are soluble and stable in the original crude oil. Structurally, asphaltenes are high-molecular-weight polycyclic organic compounds composed of aliphatic and aromatic structures.[5−7] Asphaltene adsorption can make the reservoir more oil-wet to reduce the relative permeability of the oil phase, leading to oil production reduction.[8−12] Depressurization during the oil production can cause asphaltene precipitation inside the reservoir and wellbore. The formation and wellbore blockage prevention require maintaining the pressure or applying asphaltene precipitation inhibitors during the production.[13] The asphaltene onset pressure during the depletion was extensively studied.[14] Polydispersivity, steric colloidal, aggregation, and electrokinetics are explored as the main mechanisms of asphaltene solubilization and stabilization.[15] Based on the study of the mechanisms, the solubility model, the solid model, the colloid model, and the equation of state (EOS) model are developed to describe and predict the asphaltene precipitation problems.[16]

Table 1. Formation Water Composition

	concentration (mg/L)							
pH	Ca^{2+}	Mg^{2+}	Cl^-	SO_4^{2-}	CO_3^{2-}	HCO_3^-	K^+, Na^+	TDS (mg/L)
8	14.85	7.48	2266.88	54.1	197.66	2160.08	2428.01	7156.5

Gas injection to enhance oil recovery is currently a hot research topic. The gas injection-induced deposition of asphaltenes in reservoirs is one of the main problems affecting oil recovery.[17] The tendency of asphaltene particle deposition is closely related to the complex structure of asphaltenes.[18,19] Changes in pressure, temperature, and oil composition are responsible for asphaltene precipitation.[20] Nakhli et al.[21] reveals the stability of light and heavy oils during gas injection. The average asphaltene content in immiscible produced oil is higher than that under miscible conditions.[22] Pak[23] studied the severity of asphaltene deposition under different production procedures. The severity decreases from cyclic gas injection to CO_2 injection to natural depletion. Recent studies have shown that gas injection pressure and injection volume also affect asphaltene precipitation.[24,25]

The gravimetric method,[26] viscosity measurement,[27] optical microscopy observation,[28] and light scattering measurement[29] are widely used in the asphaltene precipitation studies to find the condition that causes the asphaltene precipitation. The pressure condition is defined as AOP (asphaltene onset pressure).[30] There is no standard experimental method for measuring the amount of generated asphaltene deposits. The precipitates are collected directly under different conditions.[31,32] Asphaltene deposits precipitate at the pore throats, which reduces reservoir permeability. Researchers indirectly test the damage caused by solid precipitation in porous media.[33,34] No study can accurately measure the amount of asphaltene precipitation in porous media.

CO_2 injection-induced asphaltene precipitation is verified by interfacial tension[35] and optical methods.[36] Researchers do not have an agreement on methane injection-induced asphaltene precipitation. Some claimed that no precipitation was observed by methane injection and others did not.[31,35] Methane, CO_2, and N_2 all showed the ability to induce asphaltene precipitation in visual observation.[37] The inconsistency in the literature-reported data could be caused by the difference in the crude oil property.

Lamadian oilfield is a structural high point at the upper northern end of the Changyuan secondary structural belt in Daqing. The south and the Sartu structural high points are separated by a gentle structural saddle, an asymmetric short-axis anticline. The original gas cap is already used as underground gas storage. In the future, Lamadian oilfield is planned to be developed by the gas-assisted gravity drainage technique to produce more oil while enlarging the volume of the gas cap to increase the gas storage capacity. Therefore, any gas injection-induced formation damage must be quantified.

From the literature review above, asphaltene precipitation is experimentally studied extensively. However, most studies focus on the AOP measurement or solvent-induced asphaltene precipitation characterization. For the gas injection study, the precipitation experiments are designed as single-time gas injection following the standard swelling test. The precipitation is caused by oil compositional change. No available literature covered the asphaltene precipitation problem during the gas multiple contact process.

However, the gas injection process in the reservoir is a multiple contact process. Depending on the gas and oil properties, it could be forward or backward contacts. When the gas is injected into the formation and comes into contact with the crude oil multiple times, the composition of the reservoir fluid and the thermodynamic conditions of the system will be changed.[38,39] The original dispersed or dissolved asphaltenes lose stability or solubility and form precipitates and deposition. Therefore, this work designed a novel experimental procedure to study the asphaltene precipitation during the multiple contacts process of the methane gas injection. The physical property variation during the multiple contact process is recorded and analyzed. The core flooding experiment quantifies the formation damage caused by the asphaltene precipitation. This work could help future modeling works and field research.

2. MATERIALS

2.1. Chemicals. Sodium chloride (99.5 wt %), potassium chloride (99 wt %), magnesium chloride (98 wt %), calcium chloride (99.0 wt %), sodium carbonate (99.95 wt %), sodium bicarbonate (99 wt %), and magnesium sulfate (99%) were purchased from Sigma-Aldrich. The brine composition and the live oil properties are shown in Tables 1 and 2 correspondingly.

Table 2. Live Oil Physical Properties

oil property	value
bubble pressure (MPa)	10.4
viscosity (mPa·s)	11.92
density (g/cm³)	0.8632
gas−oil ratio (GOR) (cm³/cm³)	39

The live oil is recombined by the dead oil and associated gas collected from the Lamadian oil field. The live oil and dead oil composition is shown in Table 3. The composition of the associated gas is shown in Table 4. The temperature and pressure of the target formation in the Lamadian oil field are 45

Table 3. Oil Sample Composition

components	live oil (mol %)	dead oil (mol %)
CO_2	0.38	0
N_2	1.62	0
C_1	23.74	0
C_2	0.34	0
C_3	0.63	0
C_4	1.47	0.45
C_5	2.53	2.08
C_6	5.7	3.57
C_7	5.23	4.38
C_8	6.73	5.31
C_9	4.69	4.91
C_{10}	4.06	4.91
C_{11+}	42.88	74.39

°C and 11.4 MPa, respectively. The physical properties are listed in Table 2.

Table 4. Associated Gas Composition

components	mol %
CO_2	1.61
N_2	2.82
C_1	90.75
C_2	0.97
C_3	1.47
NC_4	1.18
IC_4	0.37
NC_5	0.52
IC_5	0.31

Methane (99.99%) and nitrogen (99.99%) were purchased from Kelong chemicals. Pentane (99.9%) was purchased from Aladin. The 0.2-micron filter paper was purchased from the Aladin.

2.2. Porous Media and Apparatus. The core flooding experiment used the real reservoir-collected core plugs. A total number of 39 pieces of core plugs were used in three core flooding experiments. The length of porous media is about 1 m, and the long core consists of several core plugs. The gaps between core plugs are filled with filter papers to reduce the capillary end effect. The permeability of the core assembly is estimated by the following eq 1[40]

$$\frac{\overline{L}}{\overline{K}} = \frac{L_1}{K_1} + \frac{L_2}{K_2} + \cdots \frac{L_i}{K_i} + \frac{L_n}{K_n} = \sum_{i=1}^{n} \frac{L_i}{K_i} \quad (1)$$

The sequence and properties of the cores used in the three experiments are shown in Table 5.

Figure 1 shows the multicontact solid-phase deposition setup. It consists of a high-temperature oven (Lianyou, operating temperature: room temperature−200 °C), displacement pump (Ruska, operating pressure: 0−70 MPa), sampler (Qianqu, volume: 1 L, operating pressure: 0−70 MPa, operating temperature: room temperature−200 °C), gas meter (Ruska, resolution: 1 mL), GC (Agilent 7890A) for gas phase and oil phase, density meter (Anton Paar), solid-phase detection system (SDS System) (Qianqu, operating pressure: 0−70 MPa, operating temperature: room temperature−200 °C), high-pressure filter (Figure 1), laser transmitter (Qianqu, Laser power: 300 mWatts, wavelength: 632.8 nm[41]), and laser receiver (Qianqu, sensitivity: 1 pWatt). The sampler is an accumulator with a piston and temperature control system that could be rotated for stirring.

Figure 2 is the experimental setup to study the impact of solid deposition on core permeability. The core flooding system is designed for 1 m-long core flooding. The injection system consisted of an injection pump (Ruska, operating pressure: 0−70 MPa), a confining pressure pump (Ruska, operating pressure: 0−70 MPa), and three accumulators (Qianqu, volume: 700 mL, operating pressure: 0−70 MPa, operating temperature: room temperature−200 °C) to hold natural gas, live oil samples, and formation water. The long core holder (Qianqu, operating pressure: 0−70 MPa, operating temperature: room temperature−200 °C) used a Teflon sleeve and a centralizer inside the cylinder to hold the 1 m-long core. The rest equipment includes a back pressure valve (Qianqu, operating pressure: 0−70 MPa, operating temperature: room temperature−200 °C), a gas meter

Table 5. Porous Media Property

parameter				
group	serial number	length (cm)	porosity (%)	permeability (mD)
1	1	8.143	28.21	545.26
	2	6.7	29.97	576.78
	3	8.2	23.43	488.3
	4	8.38	23.34	608.51
	5	7.88	23.28	440.07
	6	8.09	25.44	413.31
	7	7.71	22.85	403.05
	8	7.143	20.68	674.32
	9	8.031	26.75	387.64
	10	6.3	20.51	352.43
	11	6.53	26.04	360.04
	12	7.8	25.08	354.28
	13	7.16	27.78	1200
average permeability				521.92
2	1	7.965	21.8	1100
	2	7.933	26.28	1200
	3	8.178	25.66	1300
	4	8.16	28.66	1400
	5	7.71	22.85	403.05
	6	8.2	23.43	488.3
	7	6.7	29.97	576.78
	8	7.143	20.68	674.32
	9	8.9	26.73	620.01
	10	6.949	27.81	1400
	11	8.27	27.4	1300
	12	6.09	26.87	1400
	13	7.866	27.89	1400
average permeability				1016
3	1	7.59	25.88	2100
	2	6.243	27.5	2100
	3	9.2	24.22	2100
	4	7.17	26.8	1900
	5	7.84	20.68	2500
	6	7.38	31.36	2600
	7	8.842	16.06	1400
	8	7.65	24.22	2700
	9	8.61	28.35	1400
	10	7.72	28.59	1400
	11	7.29	25.13	1300
	12	7.15	27.72	2800
	13	7.86	30.55	2700
average permeability				2062.71

(Ruska, resolution: 1 mL), a back pressure pump (Ruska, operating pressure: 0−70 MPa), and an oven (Lianyou, operating temperature: room temperature−200 °C).

3. EXPERIMENTAL PROCEDURE

3.1. Multicontact Solid Precipitation.

(1) The live oil sample is prepared by recombining the site dead crude oil and associated gas. The live oil has a GOR of 39 m^3/m^3. Then, 500 mL of live oil sample is transferred to a 1000 mL sampler and preserved at the reservoir temperature (45 °C) and pressure (11.4 MPa).

(2) The detection chamber of the SDS system is filled with synthetic formation brine and pressurized to 11.4 MPa. Then, the formation brine is displaced by the live oil from the top of the chamber. After the
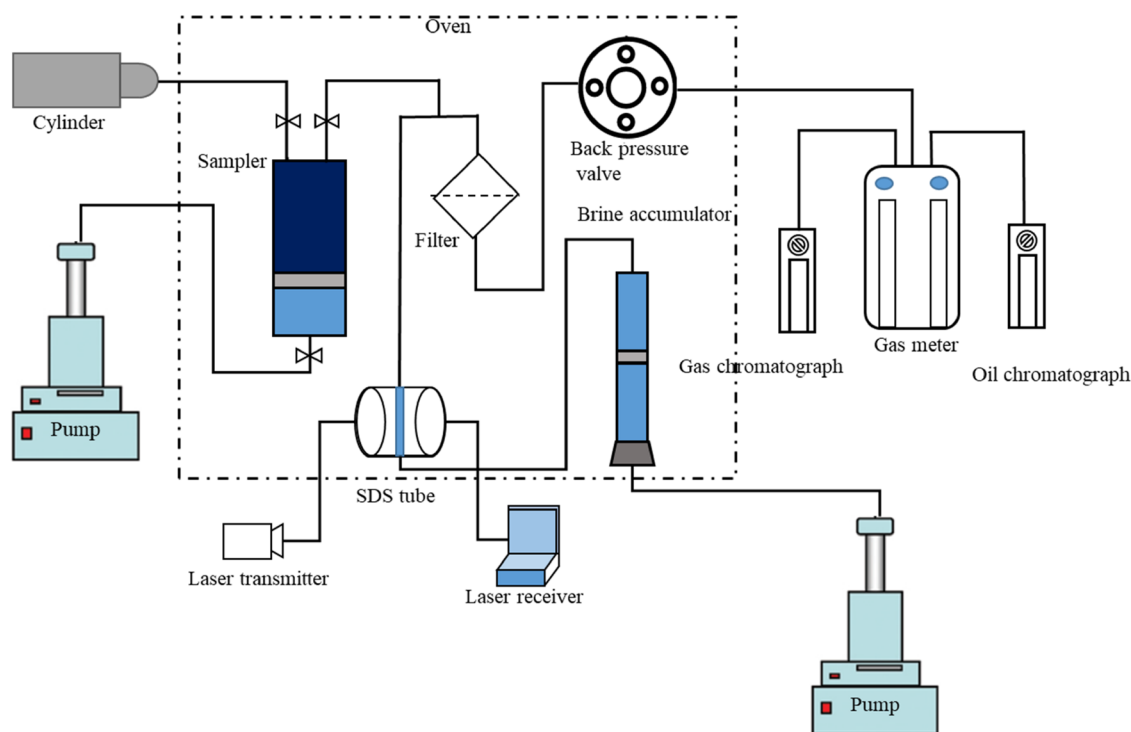
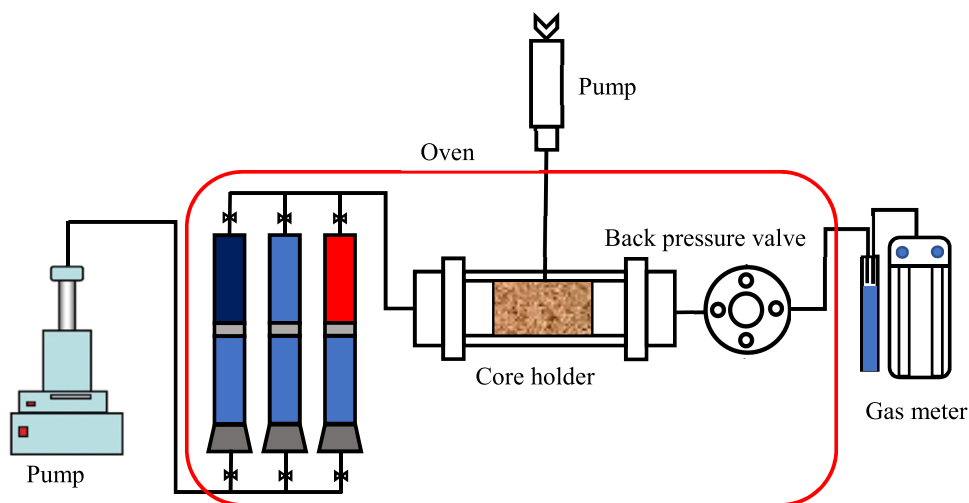**Figure 1.** Solid precipitation detection during the multiple contact process.

Figure 2. Core flooding system.

chamber is fully filled with the live oil, the laser source is turned on. One laser detector is used to record the transmitted light intensity of the sample chamber. The intensity of the crude oil without gas contact is the baseline of the experiment. After the measurement, the live oil is displaced back to the sampler by the formation brine for further gas contact. We use the mass balance method and visual checking to ensure the oil is displaced back to the sampler and the brine is not injected into the sampler.

(3) Methane is injected into the sampler and mixed with the live oil completely by rotating the sampler for 2 h. The injected gas volume is equal to the live oil volume at each injection step for experimental consistency. Then, the sampler is allowed to stand

still for two hours to reach full equilibrium. The gas phase is sampled for the GC analysis, and the rest of the gas phase is released after analysis. The pressure of the sampler is kept under reservoir condition during the experiment.

(4) Twenty milliliters of live oil is sampled for the conventional one-stage flash separation process. The separated gas and the dead oil are sampled for GC analysis, and the density of the dead oil is also recorded.

(5) The live oil sample is transferred to the detection chamber of the SDS system as the sampling procedure in step (2). The new measured transmitted light intensity is compared with the baseline. Then, steps (3)−(5) are repeated until the transmitted light intensity deviated significantly from the baseline.
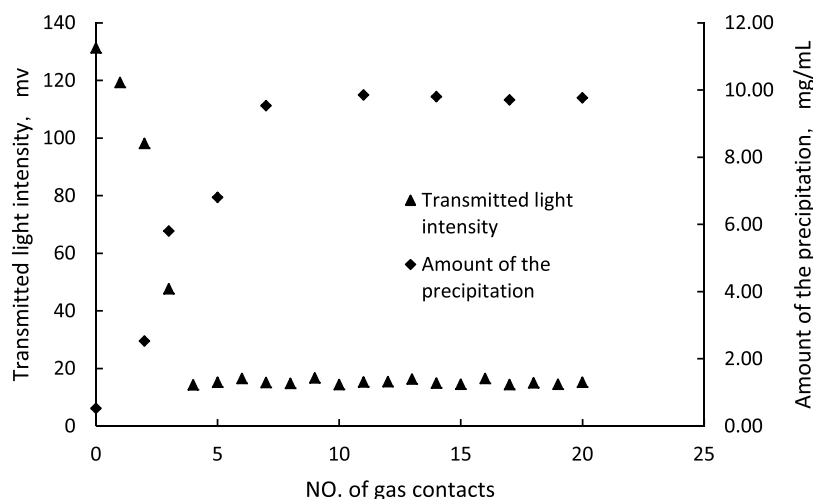
Figure 3. Transmitted light intensity and the amount of precipitation vs the number of gas contacts.
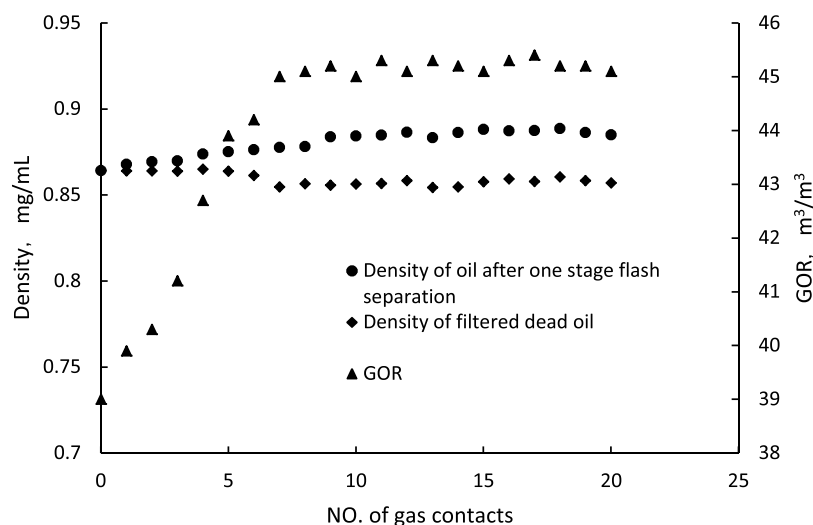

Figure 4. Physical property changes.

(6) Once the light intensity decreases significantly at a certain gas contact step, the asphaltene precipitates. The high-pressure inline filtration system is connected to the SDS chamber to collect the asphaltene precipitates. A fixed amount of live oil is filtered at reservoir pressure. Then, the filter is purged by N_2 and pentane to make sure all of the oil pass through the filter and the residue are asphaltene. The filter with residue is dried for 24 h under 56 °C. The amount of the filtered asphaltene is quantified by weight.

(7) The filtrate density is measured. The left live oil in the SDS chamber is displaced back to the sampler by brine for the next gas contact.

(8) Steps (3)−(7) are repeated 20 times.

We measure the transmitted light intensity and density for each sample multiple times. The plotted values are the average values.

3.2. Permeability Reduction Caused by Asphaltene Precipitation.

(1) After assembling the experimental instrument, according to Figure 2, the core plugs are loaded into the core holder

and evacuated. The temperature is kept to the reservoir temperature of 45 °C.

(2) The core is pressurized by the formation brine to a reservoir pressure of 11.4 MPa. Then, live oil is flooded through the core to reach the irreducible water saturation. When the GOR at the outlet of the system is 39 m^3/m^3, the pressure difference along the core $\Delta P1$ is used to calculate the relative permeability of oil phase k1.

(3) Methane is used to displace oil at a rate of 0.125 mL/min. After the injection volume reaches 4.5 HCPV, the oil recovery factor is recorded. Then, the live oil is injected at 0.125 mL/min into the core to make the gas−oil ratio 39 m^3/m^3 again. The pressure difference $\Delta P2$ across the core is recorded, and the corresponding oil phase relative permeability of k2 is calculated.

(4) The oil phase permeability before and after gas injection is used to assess the degree of reservoir damage caused by the asphaltene precipitation.

4. RESULTS AND DISCUSSION

4.1. Multicontact Asphaltene Precipitation. The single-time gas injection-caused asphaltene precipitation is studied extensively in swelling test style. The standard swelling test

design has a certain mole percentage of targeted gas injected into the crude oil sample at predetermined pressure and temperature. This experimental design does not reproduce the physical process underground since the gas flooding is a multiple contact process. Therefore, this section tries to quantify the amount of asphaltene precipitation in a multiple contact gas injection style. Moreover, the data are collected as detailed as possible to support future modeling work.

Figure 4 shows the relationship between the transmitted light intensity, the amount of precipitation, and the number of gas contacts. The experiment stopped after 20 times of methane contacts. It can be seen from the figure that the transmittance of the live oil changes significantly during the first five methane contacts. The transmitted light intensity decreased at the first methane contact. This indicated that the asphaltene started to precipitate right after the methane injection. After the fifth contact, the transmitted light intensity stopped decreasing because the amount of the dispersed asphaltene particles was high enough to make the laser detector reach its detection lower limits. We only quantify the transmitted light intensity change caused by solid precipitation. After the precipitation is formed, the size and structure of asphaltene particles might affect the transmitted light intensity in our apparatus.[42−44] The size and structure are not directly measured in this apparatus. The corresponding inline filtration result showed good agreement with the laser measurement. To be noted, the live oil sample used in the test had undissolved asphaltene without any gas contact. There were 0.53 mg/L asphaltene particles dispersed in the original oil sample. The original dispersed asphaltene particle sizes are larger than 0.2 μm. Compared with the reference light intensity and the amount of the filtered precipitates, other than flocculation and aggregation of original dispersed asphaltene particles, the dissolved asphaltene precipitated out of the crude oil at the first methane contact. Any compositional change caused by the injected gas leads to asphaltene precipitation. The maximum amount of precipitation was 9.86 mg/L after 20 contacts. After seven times of contact, the amount of precipitation reached the plateau. The amount of the deposition plateau indicated that the interaction between methane and crude oil stopped at the seventh gas contact.

Figure 4 shows the physical property changes during the gas contact process. The GOR and the density of one-stage flashed oil increased with the gas contact times. The density of the filtered oil decreased with the increase of the gas contact times. These three parameters reached a plateau at certain contact times. With the first five times of contacts, the density of one-stage flashed oil increased from 0.8641 to 0.8738 mg/mL, and the density of the filtered oil decreased from 0.8641 to 0.8638 mg/mL. After seven times of contact, as the majority of the solid-phase deposits in the crude oil are filtered out, the filtered oil density dropped significantly; it decreased to 0.8546 g/mL. The density of one-stage flashed oil did not show abrupt changes and showed a trend of increasing slowly. The filtered oil density reached a plateau at the seventh contact, and the one-stage flashed oil density reached a plateau at the 14th contact. Therefore, the structure of the asphaltene precipitates could be altered by methane after the seventh contact. A similar phenomenon is reported by the literature.[37] During the first seven contacts, the gas−oil ratio increased from the initial one-stage flash separation value of 39 m³/m³ to a stable value of about 45 m³/m³ due to the interface mass transfer between injected methane and the live crude oil. Some intermediate components were extracted by the methane, which led to an

increase in the GOR. After seven times of contact between methane and crude oil, the interaction between the formation crude oil and methane ended, and the methane and the remaining formation crude oil in the sampler were in equilibrium under the reservoir condition. No significant extraction existed after seven times of contacts. It is easy to understand that the filtered oil density reached the plateau since most of the precipitated asphaltene was filtered out by the seventh filtration. The maximum amount of asphaltene precipitation happened at the seventh contact, but the one-stage flashed oil density reached the plateau at the 14th contact. This inconsistency is an interesting phenomenon. The formed asphaltene precipitates make the fluid more compact in volume. After the asphaltene precipitation reached its maximum, the density kept increasing. This indicates that the initially existing asphaltene precipitates become more compact with no new asphaltene precipitates forming by the contact of methane. Methane acts as a solvent used in Ekulu's research.[45] Detailed structure changing[46] needs to be studied in future work.

Figure 5 shows the composition changes of one-stage flashed oil during the multiple contact process of methane injection.
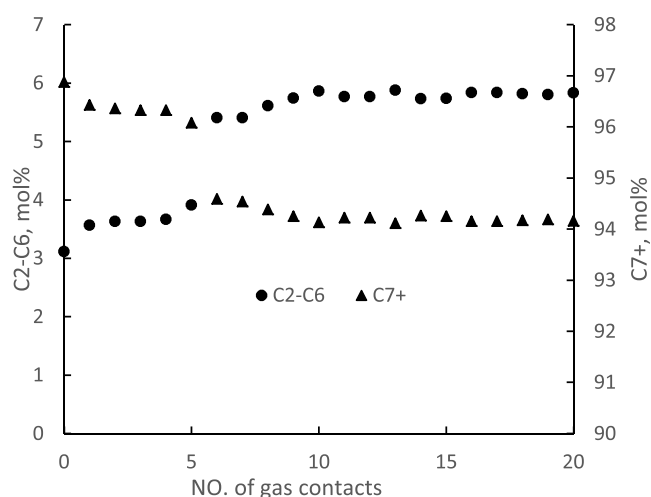

Figure 5. Composition changes of one-stage flashed oil vs contact times.

The dead oil becomes lighter than its original state in terms of composition. The C7 + concentration decreased slightly in the first five contacts with methane. With the increase in the number of contacts, it dropped sharply and stabilized after the sixth contact. The C2−C6 concentration increased accordingly. The density-changing trend of one-stage flashed oil monotonically increases from the density measurement. However, in the composition measurement, the oil becomes lighter and has an abrupt change. The inconsistency comes from the density measurement and the GC analysis difference. The density measurement used a whole oil sample while the sample of the GC analysis is filtered before the injection. Once the asphaltene precipitation is formed in the crude oil, saturates and aromatics fraction can be adsorbed onto the asphaltene precipitates. And the asphaltene prefers to adsorb heavy alkane. Therefore, C7+ shows a decrease with the increase of the contact time since there was a relatively high loss of C7+ during the filtration compared to C2−C6. This observation is consistent with the density-decreasing trend of the filtered oil in Figure 4. The abrupt drop of the density and C7+ of the filtered oil happens at the seventh and sixth methane contact, respectively. We know

from Figure 3 that the maximum amount of asphaltene precipitation happens at the seventh contact. We believe that the asphaltene agglomerates at the maximum have a distinct structure with a larger surface area leading to greater alkane adsorption. This abrupt change in the multiple contact process needs further study.

Figure 6 shows the composition changes of one-stage flashed gas in the experiment. During the continuous contact of
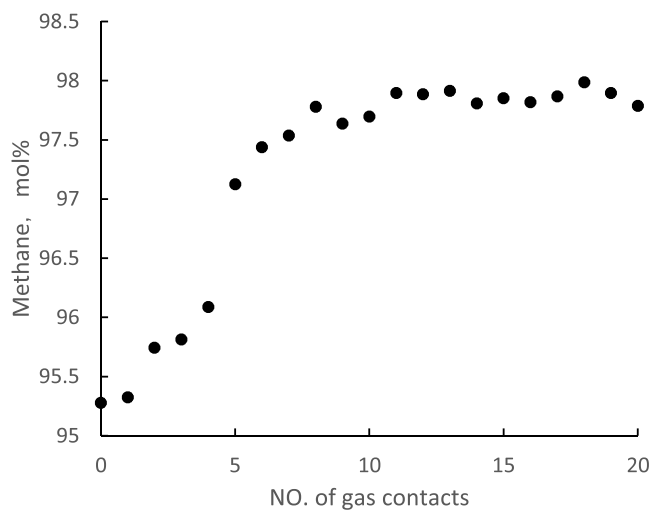

Figure 6. Composition changes of one-stage flashed gas vs contact times.

methane with the crude oil sample, due to the methane's interfacial mass transfer and extraction effect, the composition changes of one-stage flashed gas became lighter than the original separated gas. The methane content increased from 95.28 to 97.79 mol % after 20 times of contact. Before the methane contact, the original separated gas contained about 5 mol % C2−C6. The separated gas can bring some intermediate components during the one-stage flash process. With the contacts of methane, the intermediate components are extracted by methane. Therefore, the methane concentration in the separated gas increases with the increase of contact times.

Figure 7 shows the composition changes of the equilibrated gas during the methane contacts. The methane content
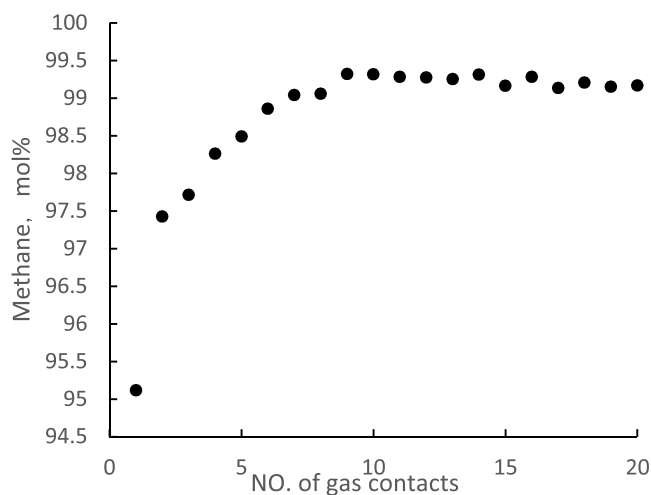

Figure 7. Composition changes of equilibrated gas vs contact times.

gradually increased from 95.11 to 99.03 mol % and was stable after the seventh contact. After 20 contacts, the methane content increased to 99.16%. The injected gas could extract intermediate components in the live oil at the first several contacts. After the seventh contact, the extraction ended, and the equilibrated gas is almost pure methane. It indicates that the extraction caused by methane contact is not strong. Compared to CO_2 injection-caused composition change,[47,48] the composition change-related asphaltene precipitation is not the primary mechanism of the crude oil used in this work. Moradi et al.[31] proved that methane shows stronger ability to induce asphaltene precipitation in crude oil than N_2 at the same mole fraction. Therefore, the minimum composition change in our experiment comes with significant methane precipitation.

Figure 8 shows the composition changes of live oil during the gas multiple contact process. The live oil composition is
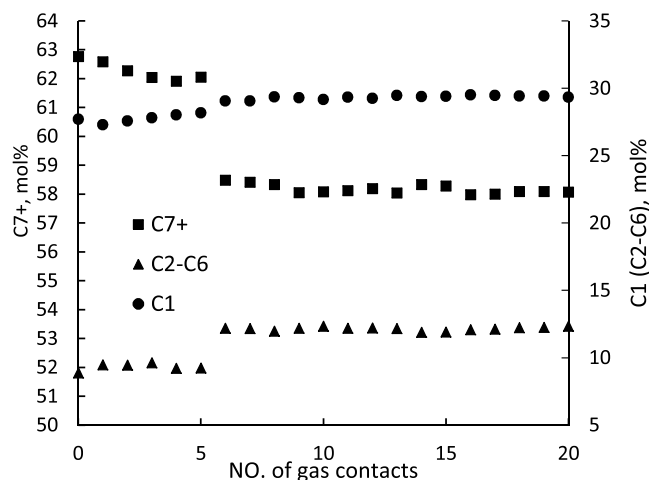

Figure 8. Composition changes of live oil vs contact times.

generated by combing the GC analysis results of the one-stage flashed gas and oil. During the first seven contacts, the content of light components C1 and intermediate C2−C6 increased as methane was injected and interacted with the crude oil. After the seventh contact, as the interaction between methane and crude oil ended, the content of each component showed no apparent change. The entire crude oil system gradually became lighter with increased injected gas contact times. After 20 contacts, the final C1 maintained at about 29.5%, C2−C6 maintained at about 12.3%, and C7 maintained at about 58.2%. This trend is similar to the result shown in Figure 5 because of the filtration. The alkene adsorbed on the filtered asphaltene precipitates was lost during the filtration. The abrupt drop only appeared on the intermediate and heavy components in the crude oil, and the methane concentration increased smoothly, which indicates that the extraction by methane was happening gradually. The gradually changed composition should not lead to an abrupt change in the precipitation property. Based on the visual observation from Zanganeh's work,[37] at constant pressure, the amount of asphaltene precipitation and the asphaltene precipitates' particle size increase with an increase of the amount of the methane injection in the single-time gas injection experiment. The methane-induced asphaltene precipitation in this work has the same mechanism as Shen's work[49] since the methane-caused extraction is proved to be weak in this work. It can be deduced that in the multiple gas contact process, the amount of asphaltene precipitation and the size of the asphaltene

precipitates caused by the methane contact. Even when the amount of asphaltene precipitation reached its maximum, the size and shape of asphaltene precipitation particles are still affected by the methane contacts. This is an apparent difference between the single-time gas injection and the multiple gas contact process. The detailed primary mechanism-related study of the asphaltene precipitation problem during the gas multiple contact process needs to be carried out in the future.

4.2. Asphaltene Precipitation-Caused Formation Damage. The amount of asphaltene precipitation during the methane injection is quantified in the previous section. However, the crude oil sample is collected from the Lamadian oil field with several high-permeability formations. Whether the methane injection-induced asphaltene precipitation causes severe formation damage or not is quantified in this section. The long core methane flooding can mimic the multiple contact process during the gas injection process in the reservoir. The bubble point pressure of the targeted oil is 10.4 MPa, and the back pressure of the core flooding test is set to be 11.4 MPa. Therefore, the injected oil can still dissolve more gas. The oil and gas are all nonwetting phases for the sandstone. Hence, the injected oil could contact the trapped gas and make the gas dissolve. And we did large pore volumes of oil injection. Therefore, the trapped gas-caused permeability reduction could be ignored.

Figure 9 shows the permeability reduction measured from the core flooding experiment. The permeability mentioned in this
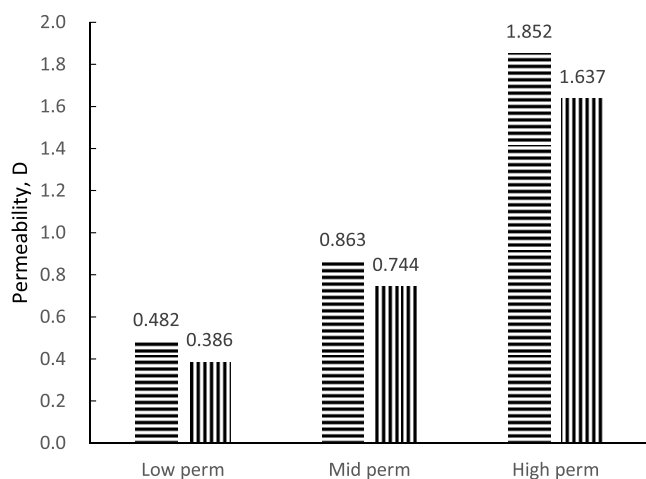
Figure 9. Permeability reduction caused by asphaltene precipitation.

section refers to the oil phase permeability at irreducible water saturation. The irreducible water saturation of the low- to high-permeability cores after oil flooding are 27.8, 25.02, and 28.07%, respectively.

The asphaltene precipitation damages all of the cores. The low-permeability core assembles' permeability decreased from 481.81 to 385.78 mD; the medium-permeability core assembles' permeability decreased from 862.75 to 743.63 mD; the high-permeability cores assembles' permeability decreased from 1852.02 to 1637.00 mD after gas injection. Even the permeability is high in the Lamadian reservoir. The asphaltene precipitation can still damage the formation. Like the sampler gas multiple contact experiments, methane gas flooding can cause asphaltene precipitation and deposition. The permeability reduction of the low-, medium-, and high-permeability core is 19.93, 13.81, and 11.61%, respectively. The asphaltene

precipitation-induced permeability reduction in this reservoir is severe. The severity of the damage increase with the decrease of the permeability since the low-permeability cores have tiny pore throats, which tend to be blocked by the asphaltene particles easier than the large pore throats. And the measured permeability is the oil phase permeability. The wettability of the core also controls the relative permeability. A low-permeability core has a larger inner surface area for the asphaltene precipitation to adsorb. Therefore, the damage severity of the low-permeability core is the highest among the three tests.

The core flooding test injects large volumes of methane to ensure that the gas and crude oil fully interact and reach equilibrium. The amount of asphaltene precipitation in the previous section is representative in the core flooding test.

Figure 10 shows the recovery after the gas injection. All tests are flooded by 4.5 hydrocarbon pore volume (HCPV). The low permeability test showed the highest recovery, while the high permeability test showed the lowest recovery with similar irreducible water saturation. The recovery of the medium and the low permeability test plateaued at about 1.8 HCPV injections. On the contrary, the low permeability test showed a two-stage recovery curve with two slopes and plateaued at 4 HCPV injection. Because the oil viscosity is high under reservoir conditions and the permeability of the core is high, the gas breakthrough happened at the 0.1 HCPV injections for all of the core flooding tests. The produced oil is collected after a gas breakthrough. The oil recovery of the first 1.8 HCPV of the medium-permeability core and the low-permeability core is similar. After the medium-permeability core flooding reached its recovery plateau, additional oil was produced at a smaller slope in the low-permeability core flooding. This extended oil production could be attributed to asphaltene precipitation. The asphaltene precipitation does not block the pore throat of the low-permeability core during the first 1.8 HCPV methane injection. Davudov et al.[50]'s research showed that particle size strongly affects the formation damage caused by asphaltene precipitation. After 1.8 HCPV gas injection, either the amount of the asphaltene precipitation is high enough, or the size of the asphaltene precipitation particles is large enough to block the pore throat. Then, the blockage of the pore throat acts as a conformance control method to divert the gas flow. The conformance effect could lead to a well-distance optimization consideration. Therefore, more oil is produced in the smaller slope after 1.8 HCPV injections. And this observation confirmed that the permeability reduction of the low-permeability core during methane injection is caused by the wettability alteration and pore throat blockage. In contrast, the permeability reduction of the medium- and high-permeability core is only caused by wettability alteration caused by the asphaltene precipitation adsorption.

5. CONCLUSIONS

(1) The newly proposed asphaltene precipitation experimental design could quantify the asphaltene precipitation in the multiple contact process.

(2) The primary asphaltene precipitation mechanism in the multiple contact process during the methane injection is not the composition change caused by the methane extraction.

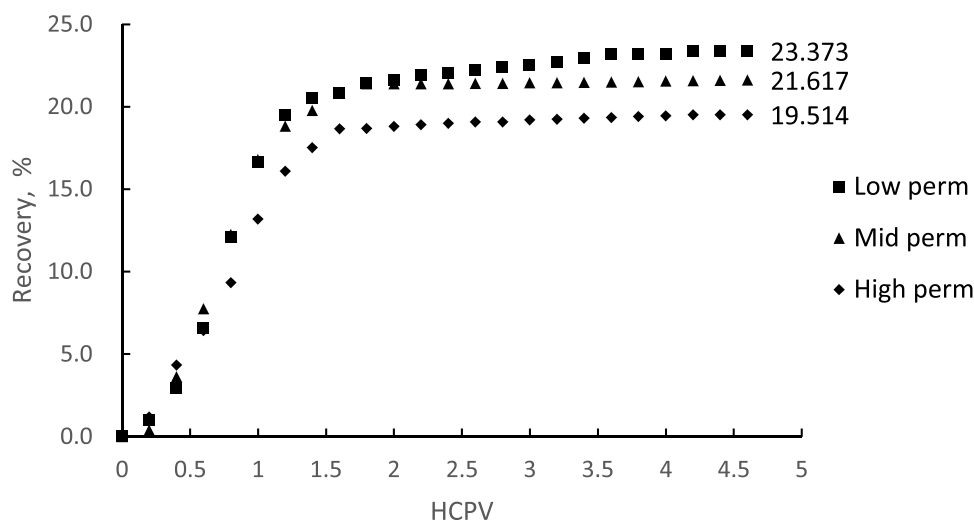(3) During the multiple contact process, after the maximum amount of asphaltene precipitation is reached, further

Figure 10. Gas injection recovery.

methane contact can still alter the structure or size of the asphaltene precipitation particles.

(4) The mechanism of permeability reduction caused by asphaltene precipitation is different depending on the porous media pore throat size and the asphaltene precipitation particle size.

(5) The asphaltene precipitation can act as a conformance control method under the right conditions.

■ AUTHOR INFORMATION

Corresponding Authors

Shuoshi Wang − *State Key Laboratory of Oil and Gas Reservoir Geology and Exploitation, Southwest Petroleum University, Chengdu 610500, China;* ⓘ orcid.org/0000-0003-2442-9824; Email: shuoshi.wang@swpu.edu.cn

Ping Guo − *State Key Laboratory of Oil and Gas Reservoir Geology and Exploitation, Southwest Petroleum University, Chengdu 610500, China;* Email: guopingswpi@vip.sina.com

Authors

He Zhang − *PetroChina Daqing Oilfield Co. Ltd, Daqing 163001, China*

Yong Liu − *Exploration and Development Research Institute of Daqing Oilfield Co. Ltd, Daqing 163001, China; Heilongjiang Provincial Key Laboratory of Reservoir Physics & Fluid Mechanics in Porous Medium, Daqing 163001, China*

Peihui Han − *Exploration and Development Research Institute of Daqing Oilfield Co. Ltd, Daqing 163001, China*

Huarong Yan − *State Key Laboratory of Oil and Gas Reservoir Geology and Exploitation, Southwest Petroleum University, Chengdu 610500, China*

Jiang Zhang − *Exploration and Development Research Institute of Daqing Oilfield Co. Ltd, Daqing 163001, China; Heilongjiang Provincial Key Laboratory of Reservoir Physics & Fluid Mechanics in Porous Medium, Daqing 163001, China*

Zhenqiang Bai − *Exploration and Development Research Institute of Daqing Oilfield Co. Ltd, Daqing 163001, China*

Zhouhua Wang − *State Key Laboratory of Oil and Gas Reservoir Geology and Exploitation, Southwest Petroleum University, Chengdu 610500, China*

Haoxiang Hukuang − *State Key Laboratory of Oil and Gas Reservoir Geology and Exploitation, Southwest Petroleum University, Chengdu 610500, China*

Xuyang Li − *State Key Laboratory of Oil and Gas Reservoir Geology and Exploitation, Southwest Petroleum University, Chengdu 610500, China*

Complete contact information is available at:
https://pubs.acs.org/10.1021/acsomega.2c05480

Notes

The authors declare no competing financial interest.

■ REFERENCES

(1) Zekri, A. Y.; Shedid, S. A.; Alkashef, H.*A Novel Technique for Treating Asphaltene Deposition Using Laser Technology*, SPE Permian Basin Oil and Gas Recovery Conference, 2001.

(2) Okabe, H.; Takahashi, S.; Mitsuishi, H.*Distribution of Asphaltene Deposition in the Rock Samples by Gas Injection*, Abu Dhabi International Petroleum Exhibition and Conference, 2010.

(3) Victorov, A. I.; Abbas, F. Thermodynamic Micellizatin Model of Asphaltene Precipitation From Petroleum Fluids. *Aiche J.* **1996**, *42*, 1753−1764.

(4) Monger, T. G.; Trujillo, D. E. Organic Deposition During Co2 and Rich-Gas Flooding. *SPE Reservoir Eng.* **1991**, *6*, 17−24.

(5) Zanganeh, P.; Dashti, H.; Ayatollahi, S. Visual Investigation and Modeling of Asphaltene Precipitation and Deposition During CO2 Miscible Injection Into Oil Reservoirs. *Fuel* **2015**, *160*, 132−139.

(6) Mansoori, G. A. A Unified Perspective On the Phase Behaviour of Petroleum Fluids. *Int. J. of Oil, Gas Coal Technol.* **2009**, *2*, 141−167.

(7) Soulgani, B. S.; Rashtchian, D.; Tohidi, B.; Jamialahmadi, M. A Novel Method for Mitigation of Asphaltene Deposition in the Wellstring. *Iran. J. Chem. Chem. Eng.* **2010**, *29*, 131−142.

(8) Yen, T. F.; et al. Investigation of the Structure of Petroleum Asphaltenes by X-Ray Diffraction. *Anal. Chem.* **2002**, *33*, 1587−1594.

(9) Soorghali, F.; Zolghadr, A.; Ayatollahi, S. Effect of Resins On Asphaltene Deposition and the Changes of Surface Properties at Different Pressures: A Microstructure Study. *Energy Fuels* **2014**, *28*, 2415−2421.

(10) Klein, G. C.; Kim, S.; Rodgers, R. P.; Marshall, A. G.; Yen, A.; Asomaning, S. Mass Spectral Analysis of Asphaltenes. I. Compositional

Differences Between Pressure-Drop and Solvent-Drop Asphaltenes Determined by Electrospray Ionization Fourier Transform Ion Cyclotron Resonance Mass Spectrometry. *Energy Fuels* **2006**, *20*, 1965−1972.

(11) Soorghali, F.; Ali, Z.; Shahab, A. Effect of Resins On Asphaltene Deposition and the Changes of Surface Properties at Different Pressures: A Microstructure Study. *Energy Fuels* **2014**, *28*, 2415−2421.

(12) Groenzin, H.; Oliver, C. M. Molecular Size and Structure of Asphaltenes From Various Sources. *Energy Fuels* **2000**, *14*, 677−684.

(13) Alimohammadi, S.; Zendehboudi, S.; James, L. A Comprehensive Review of Asphaltene Deposition in Petroleum Reservoirs: Theory, Challenges, and Tips. *Fuel* **2019**, *252*, 753−791.

(14) Buenrostro Gonzalez, E.; Lira Galeana, C.; Gil Villegas, A.; Wu, J. Asphaltene Precipitation in Crude Oils: Theory and Experiments. *AIChE J.* **2004**, *50*, 2552−2570.

(15) Bayat, M.; Mostafa, L.; Ali, Z. H.; Shahab, A. Investigation of Gas Injection Flooding Performance as Enhanced Oil Recovery Method. *J. Nat. Gas Sci. Eng.* **2016**, *29*, 37−45.

(16) Mansoori, G. A.; Vazquez, D.; Shariaty-Niassar, M. Polydispersity of Heavy Organics in Crude Oils and their Role in Oil Well Fouling. *J. Pet. Sci. Eng.* **2007**, *58*, 375−390.

(17) Zanganeh, P.; Ayatollahi, S.; Alamdari, A.; Zolghadr, A.; Dashti, H.; Kord, S. Asphaltene Deposition During Co2 Injection and Pressure Depletion: A Visual Study. *Energy Fuels* **2012**, *26*, 1412−1419.

(18) Mitchell, D. L.; Speight, J. G. The Solubility of Asphaltenes in Hydrocarbon Solvents. *Fuel* **1973**, *52*, 149−152.

(19) Speight, J. G.; Long, R. B.; Trowbridge, T. D. Factors Influencing the Separation of Asphaltenes From Heavy Petroleum Feedstocks. *Fuel* **1984**, *63*, 616−620.

(20) Hortal, A. R.; Martínez-Haya, B.; Lobato, M. D.; Pedrosa, J. M.; Lago, S. On the Determination of Molecular Weight Distributions of Asphaltenes and their Aggregates in Laser Desorption Ionization Experiments. *J. Mass Spectrom.* **2006**, *41*, 960−968.

(21) Nakhli, H.; Alizadeh, A.; Moqadam, M. S.; Afshari, S.; Kharrat, R.; Ghazanfari, M. H. Monitoring of Asphaltene Precipitation: Experimental and Modeling Study. *J. Pet. Sci. Eng.* **2011**, *78*, 384−395.

(22) Cao, M.; Gu, Y. Oil Recovery Mechanisms and Asphaltene Precipitation Phenomenon in Immiscible and Miscible Co2 Flooding Processes. *Fuel* **2013**, *109*, 157−166.

(23) Ali Mansoori, G. Modeling of Asphaltene and Other Heavy Organic Depositions. *J. Pet. Sci. Eng.* **1997**, *17*, 101−111.

(24) Bahrami, P.; Riyaz, K.; Sedigheh, M.; Yaser, A.; Lesley, J. Asphaltene Laboratory Assessment of a Heavy Onshore Reservoir During Pressure, Temperature and Composition Variations to Predict Asphaltene Onset Pressure. *Korean J. Chem. Eng.* **2015**, *32*, 316−322.

(25) King, R. W. Petroleum: Its Composition, Analysis and Processing. *Occup. Med.* **1988**, *3*, 409−430.

(26) Zendehboudi, S.; Ahmadi, M. A.; Mohammadzadeh, O.; Bahadori, A.; Chatzis, I. Thermodynamic Investigation of Asphaltene Precipitation During Primary Oil Production: Laboratory and Smart Technique. *Ind. Eng. Chem. Res.* **2013**, *52*, 6009−6031.

(27) Escobedo, J.; Mansoori, G. A. Viscometric Determination of the Onset of Asphaltene Flocculation: A Novel Method. *SPE Prod. Facil.* **1995**, *10*, 115−118.

(28) Maqbool, T.*Understanding the Kinetics of Aphaltene Precipitation From Crude Oils*, University of Michigan, 2011.

(29) Buenrostro Gonzalez, E.; Lira Galeana, C.; Gil Villegas, A.; Wu, J. Asphaltene Precipitation in Crude Oils: Theory and Experiments. *Aiche J.* **2004**, *50*, 2552−2570.

(30) Sullivan, M.; Smythe, E. J.; Fukagawa, S.; Harrison, C.; Dumont, H.; Borman, C. A Fast Measurement of Asphaltene Onset Pressure. *SPE Reserv. Eval. Eng.* **2020**, *23*, 962−978.

(31) Moradi, S.; Dabiri, M.; Dabir, B.; Rashtchian, D.; Emadi, M. A. Investigation of Asphaltene Precipitation in Miscible Gas Injection Processes: Experimental Study and Modeling. *Braz. J. Chem. Eng.* **2012**, *29*, 665−676.

(32) Zendehboudi, S.; Shafiei, A.; Bahadori, A.; James, L. A.; Elkamel, A.; Lohi, A. Asphaltene Precipitation and Deposition in Oil

Reservoirs−Technical Aspects, Experimental and Hybrid Neural Network Predictive Tools. *Chem. Eng. Res. Des.* **2014**, *92*, 857−875.

(33) Petroleum, A. S. O.*Characteristics and Impact of Asphaltene Precipitation During Co2 Injection in Sandstone and Carbonate Cores: An Investigative Analysis through Laboratory Tests and Compositional Simulation*, SPE International Improved Oil Recovery Conference in Asia Pacific, 2003.

(34) Novosad, Z.; Costain, T. G.*Experimental and Modeling Studies of Asphaltene Equilibria for a Reservoir Under CO2 Injection*, SPE Annual Technical Conference and Exhibition, 1990.

(35) Kazemzadeh, Y.; Parsaei, R.; Riazi, M. Experimental Study of Asphaltene Precipitation Prediction During Gas Injection to Oil Reservoirs by Interfacial Tension Measurement. *Colloids Surf.* **2015**, *466*, 138−146.

(36) Zanganeh, P.; Ayatollahi, S.; Alamdari, A.; Zolghadr, A.; Dashti, H.; Kord, S. Asphaltene Deposition During Co2 Injection and Pressure Depletion: A Visual Study. *Energy Fuels* **2012**, *26*, 1412−1419.

(37) Zanganeh, P.; Dashti, H.; Ayatollahi, S. Comparing the Effects of Ch4, Co2, and N2 Injection On Asphaltene Precipitation and Deposition at Reservoir Condition: A Visual and Modeling Study. *Fuel.* **2018**, *217*, 633−641.

(38) Thomas, F. B.; Bennion, D. B.; Bennion, D. W.; Hunter, B. E. Experimental and Theoretical Studies of Solids Precipitation From Reservoir Fluid. *J. Can. Pet. Technol.* **1992**, *31*, PETSOC-92-01-02.

(39) Spiecker, P. M.; Keith, L. G.; Peter, K. K. Aggregation and Solubility Behavior of Asphaltenes and their Subfractions. *J. Colloid Interface Sci.* **2003**, *267*, 176−193.

(40) Huppler, J. D. Waterflood Relative Permeabilities in Composite Cores. *J. Pet. Technol.* **1969**, *21*, 539−540.

(41) Ferworn, K. A.; Svrcek, W. Y.; Mehrotra, A. K. Measurement of Asphaltene Particle Size Distributions in Crude Oils Diluted with N-Heptane. *Ind. Eng. Chem. Res.* **1993**, *32*, 955−959.

(42) Ferworn, K. A.; Svrcek, W. Y.; Mehrotra, A. K. Measurement of Asphaltene Particle Size Distributions in Crude Oils Diluted with N-Heptane. *Ind. Eng. Chem. Res.* **1993**, *32*, 955−959.

(43) Sim, S. S.; Okatsu, K.; Takabayashi, K.; Fisher, D. B.*Asphaltene-Induced Formation Damage: Effect of Asphaltene Particle Size and Core Permeability*, SPE Annual Technical Conference and Exhibition, 2005.

(44) Mansur, C. R. E.; de Melo, A. R.; Lucas, E. F. Determination of Asphaltene Particle Size: Influence of Flocculant, Additive, and Temperature. *Energy Fuels* **2012**, *26*, 4988−4994.

(45) Ekulu, G.; Sadiki, A.; Rogalski, M. Experimental Study of Asphaltenes Flocculation Onset in Crude Oils Using the Densitometry Measurement Technique. *J. Dispersion Sci. Technol.* **2010**, *31*, 1495−1503.

(46) Zang, X.; Jian, C.; Ingersoll, S.; Li, H.; Adams, J. J.; Lu, Z.; Ferralis, N.; Grossman, J. C. Laser-Engineered Heavy Hydrocarbons: Old Materials with New Opportunities. *Sci. Adv.* **2020**, *6*, z5231.

(47) Siagian, U. W.; Grigg, R. B.*The Extraction of Hydrocarbons From Crude Oil by High Pressure Co2*, Improved Oil Recovery Symposium, 1998.

(48) Wang, P.; Zhao, F.; Hou, J.; Lu, G.; Zhang, M.; Wang, Z. Comparative Analysis of Co2, N2, and Gas Mixture Injection On Asphaltene Deposition Pressure in Reservoir Conditions. *Energies* **2018**, *11*, 2483.

(49) Shen, Z.; Sheng, J. J.*Experimental Study of Asphaltene Aggregation During Co2 and Ch4 Injection in Shale Oil Reservoirs*, SPE Improved Oil Recovery Conference, 2016.

(50) Davudov, D.; Moghanloo, R. G. A New Model for Permeability Impairment Due to Asphaltene Deposition. *Fuel* **2019**, *235*, 239−248.